

# Aspects of electron transport through a quantum dot

R. Taranko, M. Krawiec, T. Kwapiński, E. Taranko,  
 K. I. Wysokiński

Institute of Physics and Nanotechnology Center,  
 Maria Curie-Skłodowska University,  
 Pl. Marii Curie-Skłodowskiej 1, 20-031 Lublin, Poland  
 (Dated: October 26, 2018)

The work of the Lublin group on the non-equilibrium transport through the quantum dot coupled to external leads (normal or superconducting) and subject to external time dependent fields has been reviewed.

## I. INTRODUCTION

This paper is an extended version of the talk given at the LFPPI-network conference in Łódź (Poland). It makes extensive use of our published work [1]-[9]. In particular all figures which appear in the present review have already been presented there.

Due to recent developments in fabrication of small electronic devices equilibrium and non-equilibrium properties of mesoscopic systems have been of great interest during last decade. In particular a lot of work has been done on electron transport through quantum dots.

The quantum dots are small pieces of matter containing few to few tens of electrons. Very often they are electrically defined in a two dimensional electron gas placed at the interface in GaAs-GaAlAs heterostructure. The important point about quantum dots is that they can be viewed like impurities in solids [10] but at the same time their coupling to external environment can be controlled and the nonequilibrium transport[11] can be studied.

The discovery of the Kondo effect in quantum dots [12, 13] connected to external leads by tunnel junctions has resulted in increased experimental and theoretical interest. The Kondo effect in quantum dots manifests itself as an increased conductance  $G$  of the system at temperatures lower than the Kondo temperature  $T_K$ . It is due to formation of the so-called Abrikosov-Suhl or Kondo resonance at the Fermi energy. This is a many-body singlet state involving spin on the quantum dot and electrons in the leads.

Here we review our studies of stationary nonequilibrium transport with help of Keldysh Green's function formalism. To obtain the information about the time dependent phenomena in a quantum dots which parameters do depend on time we calculate the time evolution operator and then time dependent charge and current.

## II. TIME-INDEPENDENT TRANSPORT

In this section we shall present the results for time independent transport through quantum dot with a single energy level. We start with asymmetrically coupled quantum dot (section II.A), discuss the role of Van Hove singularity in the density of states of the electrodes (section II.B) and consider the dot coupled to one normal and other superconducting lead (section II.C).

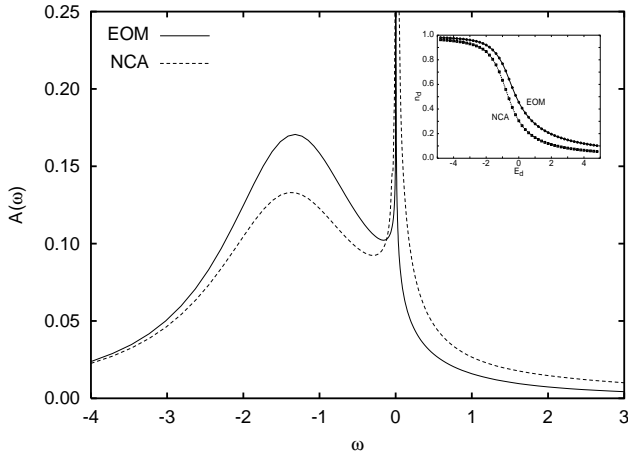


FIG. 1: The equilibrium density of states on the quantum dot obtained within *EOM* (solid line) and *NCA* (dashed line). Note the relative shift of the spectral weight with respect to the chemical potential  $\mu = 0$  which results in different occupations shown in the inset. The parameters are:  $E_d = -2$ ,  $\Gamma_L = \Gamma_R = 1$  and  $T = 10^{-3}$ . [2]

### A. Non-equilibrium Kondo effect in asymmetrically coupled quantum dots

It is well known that in systems containing quantum dot the Kondo effect manifests itself (at low temperatures) as an enhancement of the conductance at zero source-drain voltage[10],  $V_{SD} = 0$ . Occasionally the Kondo peak in conductance appearing at non-zero voltages  $V_{SD} \neq 0$  has been observed [14, 15], the so called anomalous Kondo effect. This phenomenon has been investigated experimentally for the dot coupled weakly to one and strongly to the other lead. It was observed that the source-drain voltage, at which the peak appeared, scales roughly linearly with a gate voltage  $V_g$ . Performing model calculations based on non-equilibrium transport theory we have found that the emergence of the Kondo peak at non-zero voltages is caused by asymmetric coupling to external leads.

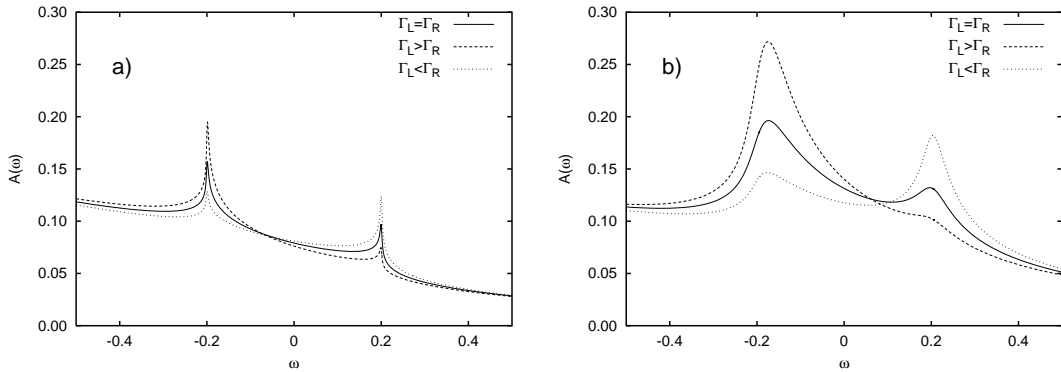


FIG. 2: The non-equilibrium density of states obtained within a) - *EOM* and b) - *NCA* for the symmetric  $\Gamma_L = \Gamma_R$  (solid lines) and asymmetrically coupled quantum dot with  $\Gamma_L = 2\Gamma_R$  (dashed) and  $\Gamma_L = \frac{1}{2}\Gamma_R$  (dotted lines).  $\mu_R = -\mu_L = 0.2$  and the other parameters are the same as in Fig. (1). [2]

The system under consideration is described by single impurity Anderson model and the Landauer-

type formula for the current flowing in the system, left lead - quantum dot - right lead is [11]

$$J = \frac{e}{\hbar} \sum_{\sigma} \int d\epsilon \frac{\Gamma_L^{\sigma}(\epsilon) \Gamma_R^{\sigma}(\epsilon)}{\Gamma_L^{\sigma}(\epsilon) + \Gamma_R^{\sigma}(\epsilon)} \left( -\frac{1}{\pi} \text{Im} G_{\sigma}^r(\epsilon) [f_L(\epsilon) - f_R(\epsilon)] \right) \quad (1)$$

where  $f_{L/R}(\epsilon)$  denotes the Fermi distribution function,  $G_{\sigma}^r(\epsilon)$  - retarded on-dot Green's function and  $\Gamma_{L/R}^{\sigma}(\epsilon)$  - effective coupling of the localized electrons to the conduction band.

The retarded Green's function required for the calculations of the tunneling current and the differential conductance of the system is obtained within the equation of motion (*EOM*) technique with slave boson representation of the electron operators and non-crossing approximation (*NCA*). In both cases we assume  $U \rightarrow \infty$ . As we have checked, the *EOM* method gives correct position of the Kondo peak, however it leads to incorrect width of the peak and occupation on the dot. Therefore we have used *NCA* technique which is generally accepted for description of the system in the Kondo regime.

In the Fig.1 we present the equilibrium density of states (*DOS*) of the quantum dot coupled to two leads obtained by means of the *NCA* and *EOM* approaches. The main features of the *DOS* remain the same in both cases. However the height and width of the Kondo peak are much larger in *NCA*.

Fig.2 gives the non-equilibrium *DOS* obtained for symmetric ( $\Gamma_L = \Gamma_R$ ) and asymmetric couplings  $\Gamma_L = 2\Gamma_R$  and  $\Gamma_L = \frac{1}{2}\Gamma_R$ . We see that the Kondo peak is always located at energies coinciding with those of the Fermi levels of the leads [11]. Thus in non-equilibrium we get two Kondo resonances in the *DOS* pinned to the Fermi energies of corresponding leads.

The differential conductance spectrum of the same system is shown in the Fig.3. For comparison

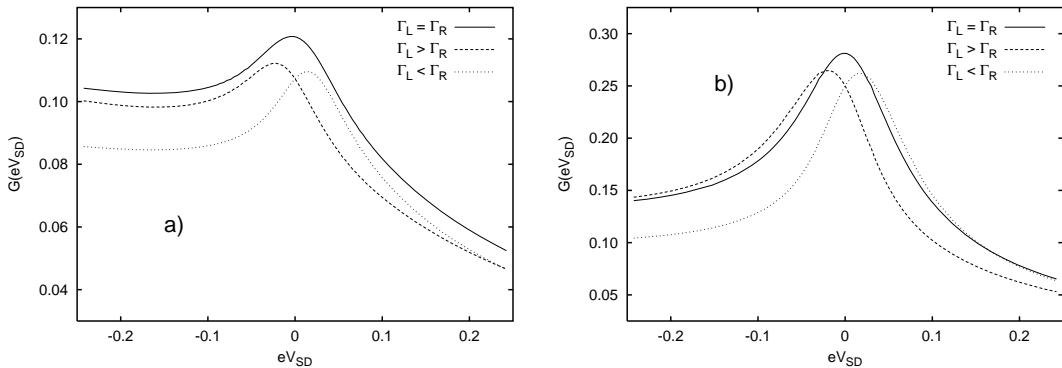


FIG. 3: The differential conductance ( $G(eV_{SD}) = dJ/d(eV_{SD})$ ) obtained within *a*) - *EOM* and *b*) - *NCA* for the symmetric  $\Gamma_L = \Gamma_R$  (solid lines) and asymmetrically coupled quantum dot with  $\Gamma_L = 2\Gamma_R$  (dashed) and  $\Gamma_L = \frac{1}{2}\Gamma_R$  (dotted lines). [2]

we have also plotted the conductance of the symmetrically coupled quantum dot. In the symmetric case ( $\Gamma_L = \Gamma_R$ ) the Kondo peak is located exactly at zero bias ( $V_{SD} = 0$ ) but for  $\Gamma_L > \Gamma_R$  ( $\Gamma_L < \Gamma_R$ ) it is shifted to the negative (positive) voltages. This finding is in nice qualitative agreement with experimental situation in transport through the quantum dot in the presence of asymmetric barriers. Further details regarding this anomalous Kondo effect can be found in [2].

## B. Van Hove singularities and the Kondo effect

Here we present some results regarding influence of the band structure of the leads, in particular Van Hove singularities in the *DOS* on the tunneling current through the quantum dot. We have assumed the conduction electron energies of the leads in the form characteristic for two-dimensional

tight-binding spectrum which is known to possess the logarithmic singularity in the middle of the band. To calculate the retarded Green's function we have used Hubbard I type decoupling and performed calculations of the density of states (DOS) on the dot and the differential conductance through it. To see the influence of spectrum of the electrode on transport we repeated the calculations for constant, Lorentzian and Van Hove singular *DOS*.

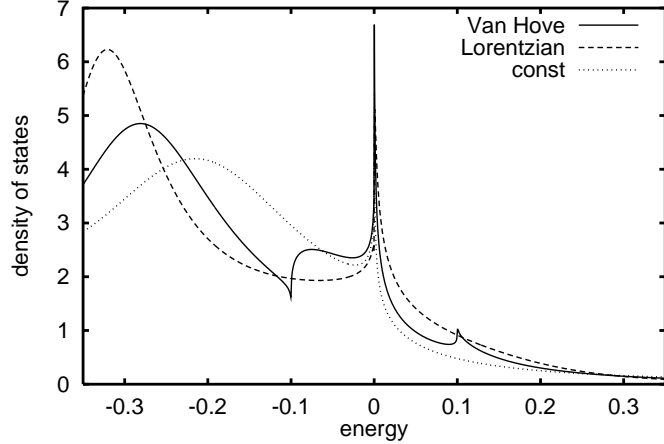


FIG. 4: The density of states on the dot calculated for  $V = 0.1W$ ,  $T = 10^{-4}W$  ( $W$  is the bandwidth) and for three different spectra of electrons in the leads. Note the structure due to Van Hove singularities and robustness of the coherent (Kondo) feature at the Fermi level. [7]

Fig. 4 shows the effect of the Van Hove singularity in the leads on the density of states of the electrons on the dot and figure 5 shows the corresponding differential conductance spectra. One

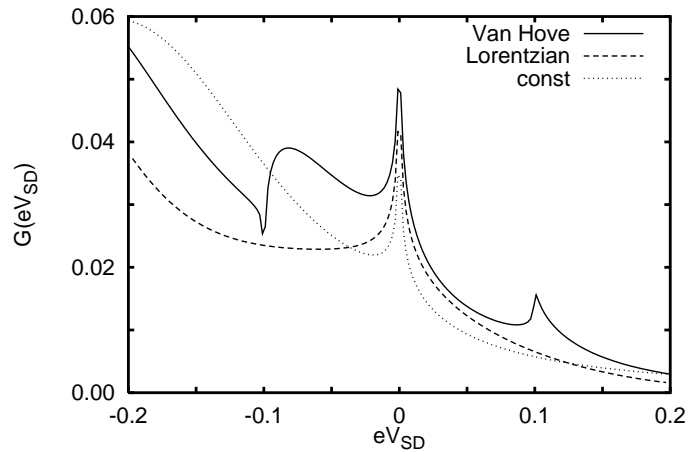


FIG. 5: The differential conductance  $G$  (in units of  $e^2/h$ ) for three spectra of electrons in the leads. The Van Hove singularity affects the conductance and produces additional structure around the Fermi level. [7]

observes marked changes of the tunneling current and the differential conductance due to the Van Hove singularities (now shifted by  $\pm 0.05W$ ). The dip seen below Fermi level ( $\mu_L - \mu_R < 0$ ) is due to the real part of the self-energy, while the Kondo like structure above the Fermi level (solid curve) is connected with the imaginary part, which is proportional to the lead *DOS*. The structure thus reflects the presence of Van Hove singularity in the spectrum of carriers in the leads.

### C. Electron transport through a quantum dot coupled to normal metal and superconductor

Here we present some of the results of our studies concerning transport properties of the quantum dot coupled to the normal metal and *BCS*-like superconductor ( $N - QD - S$ ) in the presence of the Kondo effect and Andreev scattering. The system is described by single impurity Anderson model in the limit of strong on-dot interaction. We have used *EOM* method to calculate non-equilibrium Green's functions together with the modified slave boson technique. The details of calculations can be found in [8] and here we present the results for the quantum dot *DOS* only, as it gives valuable information about the system.

In Fig. 6 we show the *DOS* of the quantum dot for various positions of the dot energy level  $E_d$ . Clearly, the Kondo effect manifests itself in the resonance at the Fermi energy which survives the

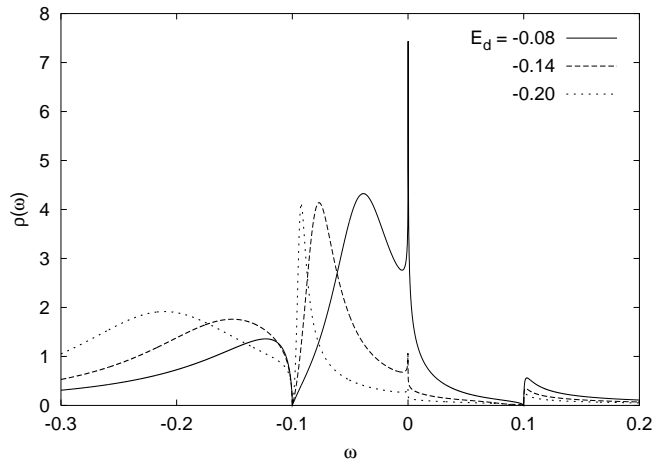


FIG. 6: The density of states of the quantum dot in  $N - QD - S$  system for various values of the dot energy level  $E_d$ . Other parameters are following:  $\Gamma_N = \Gamma_S = 0.02$ ,  $\Delta = 0.1$ ,  $eV = 0$ ,  $T = 10^{-5}$  in the units of the bandwidth  $W$ . [8]

presence of superconductivity in one electrode. The additional structure at  $\omega = \pm\Delta = \pm0.1$  reflects the superconducting gap  $\Delta$ .

In the next step we consider *DOS* in the non-equilibrium situation ( $eV = \mu_N - \mu_S \neq 0$ ). Recall that in the  $N - QD - N$  system for  $eV \neq 0$  there emerge two resonances pinned to Fermi levels of the left and right leads, respectively. In the present case there is a gap in the spectrum of the superconducting lead and we observe only one resonance pinned to the normal metal Fermi level ( $\mu_N$ ) (see Fig. 7). The presence of one superconducting electrode opens a possibility for the Andreev reflections. This is process in which an electron coming to the N-S interface from the normal metal side is reflected back into metal as hole, while the Cooper pair enters the superconductor. From the general expression for the nonequilibrium current (1) in the  $N - QD - S$  system one expects the Kondo peak in the tunneling mediated by the Andreev reflections. The corresponding part of the total current is written in the form [8]

$$J_A = -\frac{2e}{h} \int_{-\infty}^{\infty} \frac{d\omega}{2\pi} T_{NS}^A(\omega) [f(\omega - eV) - f(\omega + eV)], \quad (2)$$

where we have introduced "transmittance"  $T_{NS}^A(\omega)$  associated with the Andreev tunneling. At zero temperature and at energies less than the superconducting gap,  $T_{NS}^A(\omega)$  can be regarded as a total transmittance because Andreev tunneling is the only process allowed in these circumstances.  $T_{NS}^A(\omega)$  for different values of the  $eV$  is plotted in the Fig.8. The broad resonances at  $\omega \approx \pm 0.06$  are

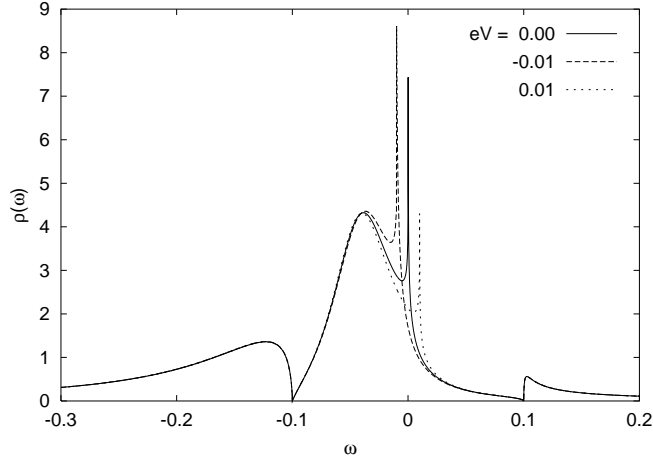


FIG. 7: Equilibrium ( $eV = 0$ ) and non-equilibrium ( $eV = \pm 0.01$ ) density of states of the quantum dot in the  $N - QD - S$  system. Other parameters have following values:  $\Gamma_N = \Gamma_S = 0.02$ ,  $\Delta = 0.1$ ,  $E_d = -0.08$ ,  $T = 10^{-5}$  in units of the bandwidth  $W$ . [8]

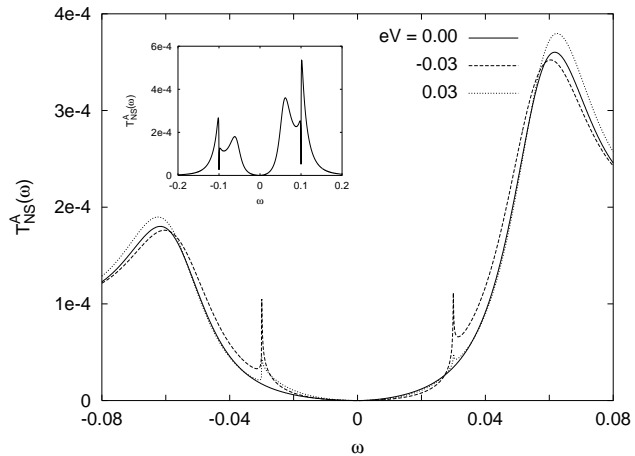


FIG. 8:  $T_{NS}^A(\omega)$  for different values of the bias voltage  $eV = 0$  (solid line),  $-0.03$  (dashed) and  $0.03$  (dotted line).  $E_d = -0.08$ ,  $\Gamma_N = \Gamma_S = 0.01$  and  $\Delta = 0.1$ . Inset: large scale view of the equilibrium  $T_{NS}^A(\omega)$  [8].

reflections of the dot energy level  $E_d = 0.08$  for electrons and holes, shifted from its original position due to renormalization caused by the strong Coulomb interaction. The important point is that there is no Kondo peak in equilibrium ( $eV = 0$ ) transmittance. However as soon as we go away from the  $eV = 0$ , we can observe the Kondo peaks at energies  $\omega = \pm eV$  and the strong asymmetry between negative (dashed line) and positive (dotted line) voltages. While in the former case we have very well resolved resonances, in the latter these resonances are strongly suppressed. This asymmetry is strictly related to the density of states (see Fig. (6)), where we also observe such asymmetry.

Since equilibrium transmittance  $T_{NS}^A(\omega)$  does not show the Kondo peak, we cannot expect it in the differential conductance  $G_A(eV_{SD}) = dJ_A/d(eV_{SD})$  with  $J_A$  defined by (2). It turns out that  $G_A(eV_{SD})$  is very sensitive to the position of the dot energy level (see Fig. 7 in ref. [8]). More detailed discussion of these results can be found in Ref. [8].

### III. TIME-DEPENDENT TRANSPORT

In this section we consider the transport properties of a quantum dot (QD) under the influence of external time-dependent fields. The high-frequency signals may be applied to a QD and the time-dependent fields will modify the tunneling current. New effects have been observed and theoretically described, e.g. photon-assisted tunneling through small quantum dots with well-resolved discrete energy states [16, 17, 18], photon-electron pumps [19, 20, 21] and others. One can investigate the current flowing through a QD under periodic modulation of the QD electronic structure [22] or periodic (non-periodic) modulation of the tunneling barriers [21] and electron energy levels in both (left and right) electron reservoirs [23].

We consider the simplest case of the quantum dot with multiple energy levels without the electron-electron Coulomb interaction coupled to two leads (right and left) in the presence of external microwave (MW) fields which act on all parts of the system. Under the adiabatic approximation the single-electron energies of the time dependent driven system can be represented in the form  $\varepsilon_{\vec{k}}(t) = \varepsilon_{\vec{k}_0} + \Delta \cos \omega t$ . We describe the dynamical evolution of the charge localized on the QD and the current flowing through the system in terms of the time evolution operator (for details see Refs [1,3,9,24].

In the first subsection we consider the influence of the band structure of the leads on electron transport through the QD and in the next subsection we consider the time-dependent transport through the QD with additional tunneling channel.

#### A. Band structure effects in time-dependent electron transport through the QD

Here we are going to study the influence of the singularities of the leads band structure and therefore we are forced to go beyond WBL. Within the formalism of the non-equilibrium Green's functions it is extremely difficult to calculate, e.g. the time dependent current  $j_L(t)$  tunneling from the left lead to the QD. We recall that the general formula for the current flowing e.g. from the left lead into the QD is usually expressed in terms of the QD retarded Green function  $G^r(t, t_1)$ . However,  $G^r(t, t_1)$  satisfies the Dyson equation with subsequent double time integrations and for the time-dependent Hamiltonian it is a very difficult task to calculate it. Therefore, in the following, we calculate the QD charge and current using the evolution operator method. The potential drop between the left and right leads is given by  $\mu_L - \mu_R = eV_{s-d}$  and  $V_{s-d}$  is the measured voltage between source and drain. In experiments the gate voltage controls the position of QD's energy level  $\epsilon_d$  and to mimic measurements of the QD charge or current vs gate voltage we have calculated them against  $\epsilon_d$ . To study the effect of the leads band structure on the electron transport through the QD, we have assumed the two-dimensional tight binding simple cubic crystal spectrum (2D-TB) for leads conduction electrons, which is known to possess the logarithmic singularity in the middle of the band.

In Fig. 9 in the left panels we show the time-averaged QD charge, tunneling current and the derivative of the tunneling current with respect to the QD energy level  $\epsilon_d$ . In the right panels the corresponding differences ( $\Delta\langle n(t) \rangle$ ,  $\Delta\langle j_L(t) \rangle$  and  $\Delta\langle dj_L \rangle / d\epsilon_d$ ) between the results obtained for 2D-TB leads DOS and obtained within wide-band limit (WBL) usually used in literature are given. The dashed lines correspond to the static case ( $\omega = 0$ ) and the solid lines correspond to the time-dependent transport.

One can see, that, e.g. for  $\epsilon_d = 1$ , the tunneling current calculated for 2D-TB leads DOS is greater than that obtained within WBL up to a factor of  $\sim 0.30$  whilst for  $\epsilon_d = 1$  up to  $\sim 1.50$  for the static case and this difference decreases with increasing amplitude  $\Delta_L$  ( $\Delta_d = \Delta_L/2$ ,  $\Delta_R = 0$ ). It is

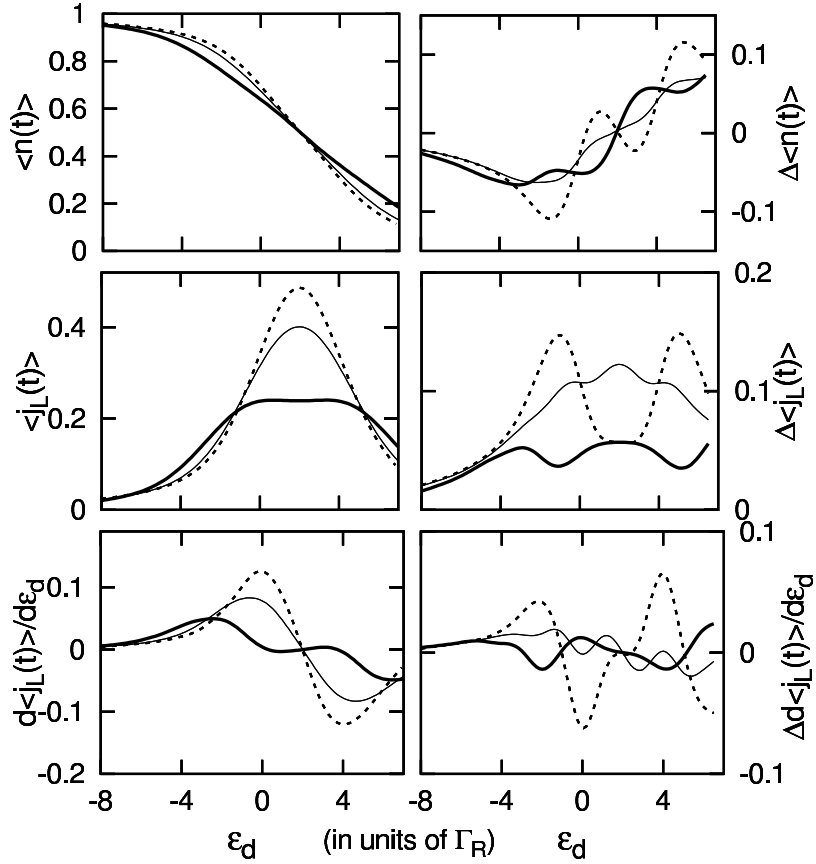


FIG. 9: The time averaged QD charge  $\langle n(t) \rangle$ , tunneling current  $\langle j_L(t) \rangle$  and derivative  $d\langle j_L(t) \rangle / d\epsilon_d$  (in arb. units) vs  $\epsilon_d$  obtained for 2D-TB leads DOS - the left panels. In the right panels the corresponding differences between the results showed in left panels and those obtained within WBL ( $\Delta\langle n(t) \rangle$ ,  $\Delta\langle j_L(t) \rangle$  and  $\Delta\langle d\langle j_L(t) \rangle / d\epsilon_d \rangle$ ) are given. The thick (thin) curves correspond to  $\Delta_L = 8$ ,  $\Delta_d = 4$ ,  $\Delta_R = 0$  ( $\Delta_L = 4$ ,  $\Delta_d = 2$ ,  $\Delta_R = 0$ ) and  $\omega = 2$ ,  $\mu_R = 0$ ,  $\mu_L = 4$ . The dashed curves correspond to the time-independent case. [3]

interesting that the  $\Delta\langle j_L(t) \rangle$  curves for different  $\Delta_L$  exhibit local minima or maxima at the same  $\epsilon_d$ . For example,  $\Delta\langle j_L(t) \rangle$  for the static case possesses a local minimum for  $\epsilon_d = 2$  (the middle point between the chemical potentials  $\mu_L$  and  $\mu_R$ ) but for the time-dependent case we observe local maxima, greater for  $\Delta_L = 4$  and lesser for greater amplitude  $\Delta_L = 8$ . The bottom panels show the derivative  $d\langle j_L(t) \rangle / d\epsilon_d$  vs  $\epsilon_d$  and the corresponding differences obtained for two considered models of the leads DOS. As before, the greatest differences are observed for the static case (dashed lines) for QD energy levels  $\epsilon_d$  equal to the chemical potentials  $\mu_L$  or  $\mu_R$ . For the time-dependent transport these differences are much smaller and hardly depend on amplitudes  $\Delta_L$  and  $\Delta_d$ , contrary to  $\Delta\langle j_L(t) \rangle$  which are greater for smaller values of  $\Delta_L$  and  $\Delta_d$ .

In the next step we consider the influence of the lead DOS structure on the photon-assisted tunneling through a quantum dot. In experiment, in average current vs gate voltage curve, a "shoulder" is observed on the left side of the main resonant peak for the case of a MW field applied on one lead only. In Fig.10 we compare the structure of the main resonant peak in the average current  $\langle j_L(t) \rangle$  and the derivative  $d\langle j_L \rangle / d\epsilon_d$  plotted vs  $\epsilon_d$  obtained within WBL (right panels) and calculated for 2D-TB leads DOS (left panels) at half-filled bands. The remarkable differences are visible for negative values of  $\epsilon_d$ . The main resonant peaks are broader and lower and their height is almost independent on the amplitude  $\Delta_R$ . The photon-assisted tunneling for  $\epsilon_d = \pm 1$  is clearly visible (lower panels of Fig.10).

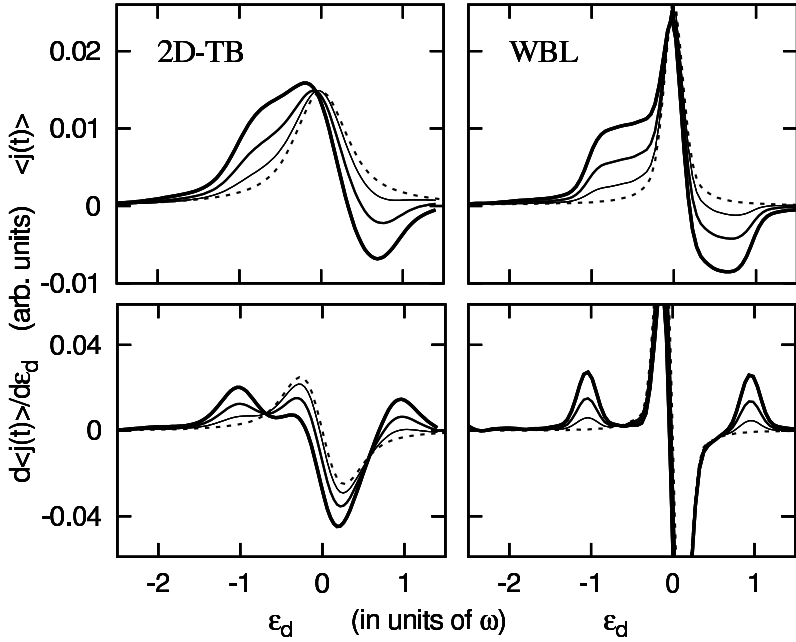


FIG. 10: Left panels - the average current  $\langle j_L(t) \rangle$  and derivative  $d\langle j_L(t) \rangle/d\epsilon_d$  vs  $\epsilon_d$  for external field applied only to the right lead in the case of the 2D-TB leads DOS. The solid curves correspond to  $\Delta_R/\omega = 0.3$  (thin lines), 0.5 and 0.7 (thick lines). The dotted curve is the resonant peak without external field. The parameters are  $\Gamma_L = \Gamma_R = 0.1\omega$  and  $\mu_L = -\mu_R = 0.05\omega$ . For comparison, on the right panels the same as on the left but obtained within WBL. [3]

### B. Electron transport through a QD in the presence of a direct tunneling between leads

The progress of nanomaterials science has enabled the experimental study of the phase coherence of the charge carriers in many mesoscopic systems. Especially, the Fano resonances in the conductance were observed [25], which imply that there are two paths for transfer of electrons between a source and a drain. The recent experimental and theoretical study with a low-temperature scanning tunneling microscope (STM) of the single magnetic atom deposited on a metallic surface showed also the asymmetric Fano resonances in the tunneling spectra [25, 26, 27, 28]. The STM measurements indicate that in tunneling of electrons between STM tip and a surface with a single impurity atom two different paths are present. The electrons can tunnel between the tip and the adsorbate state and directly between the tip and the metal surface.

In this subsection we address the issue of a QD with a bridge channel between a source and a drain driven out of equilibrium by means of a dc voltage bias and additional time-dependent external fields.

We model the QD coupled to the left and right electron reservoirs with the additional bridge tunneling channel between them (represented by the coupling  $V_{LR}$ ) by the usually used Anderson-type Hamiltonian where  $U = 0$ .

Here we show the numerical results of the time-averaged current  $\langle j_L(t) \rangle$  and its derivatives with respect to the QD energy level position and the chemical potential  $\mu_L$  (or equivalently, with respect to the gate and source-drain voltages) for different sets of parameters which characterize our system.

At first, we consider the dependence of  $\langle j_L(t) \rangle$  vs.  $\epsilon_d$  for given values of the left lead chemical potential  $\mu_L$ . In Fig. 11 we present such curves for different values of  $\mu_L$  obtained for  $\mu_L = 8$ . The left (right) panel corresponds to  $V_{RL} = 0$  ( $V_{RL} = 10$ ). In the case of vanishing over-dot tunneling channel (the left panel) the current has a simple structure – a single peak localized in the middle

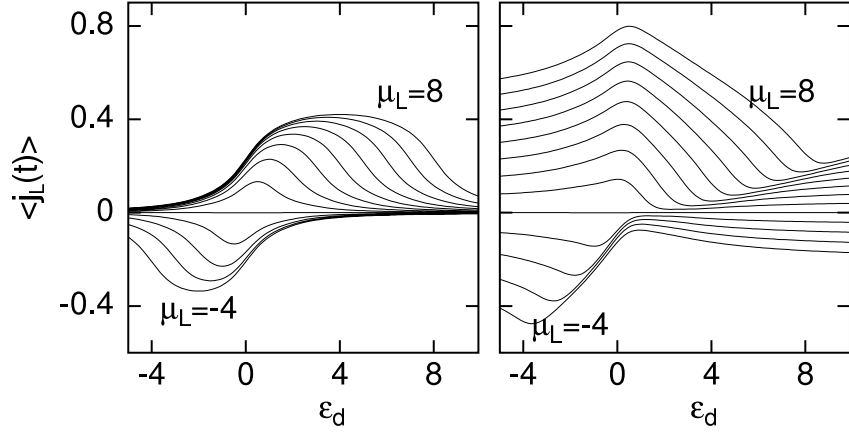


FIG. 11: The average current  $\langle j_L(t) \rangle$  against  $\varepsilon_d$  for given values of  $\mu_L$  (beginning from  $\mu_L = -4$  up to  $\mu_L = 8$ ). The left and right panels correspond to  $V_{RL} = 0$  and  $V_{RL} = 10$ , respectively,  $\mu_R = 0$ ,  $V = 4$ ,  $\Delta_L = 2$ ,  $\Delta_d = 1$ ,  $\Delta_R = 0$ ,  $\omega = 2$ . [9]

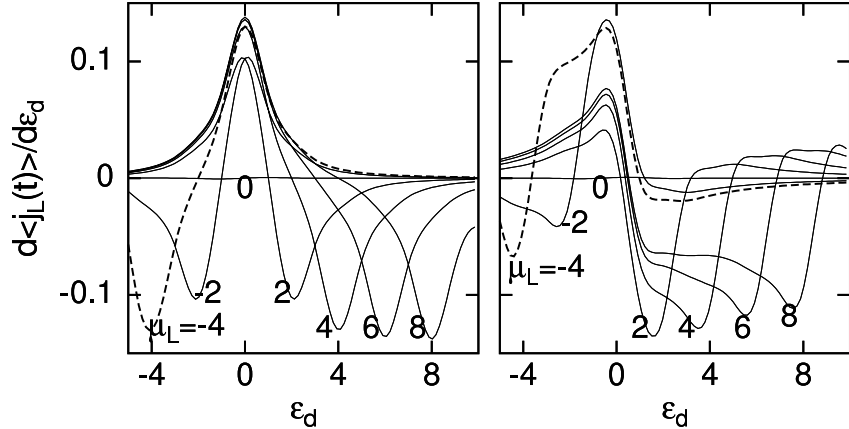


FIG. 12: The derivatives of the average current against  $\varepsilon_d$  with respect to the QD energy level  $\varepsilon_d$ ,  $d\langle j_L(t) \rangle/d\varepsilon_d$ , for given values of  $\mu_L$  (beginning from  $\mu_L = -4$  up to  $\mu_L = 8$ ). The broken curves correspond to  $\mu_L = -4$ . The left (right) panel corresponds to  $V_{RL} = 0$  ( $V_{RL} = 10$ ) and the other parameters as in Fig. 11. [9].

between  $\mu_L$  and  $\mu_R$  for smaller values of  $\mu_L$ . The width of this peak increases with increasing  $|\mu_L|$  and for greater values of  $|\mu_L|$  the current is almost independent of  $\varepsilon_d$  localized inside the energy region between  $\mu_R$  and  $\mu_L$ . For non-vanishing over-dot tunneling (Fig. 11, the right panel) the curves  $\langle j_L(t) \rangle$  become asymmetric. With increasing source-drain bias, the current possesses greater values in comparison with the  $V_{RL} = 0$  case due to the direct tunneling between both leads. Note, however, that due to the interference effects the resulting  $\langle j_L(t) \rangle$  curves are asymmetric. The interference effects are most visible for  $\varepsilon_d$  lying approximately in the region  $(\mu_R, \mu_L)$ .

In Fig. 12 we show the derivatives of the average current vs. the QD energy level  $\varepsilon_d$  obtained for some values of  $\mu_L$ . There are the results of the differentiation of curves shown in Fig. 11. Again, the most visible differences between the results obtained for  $V_{RL} = 0$  and  $V_{RL} \neq 0$  are present for the QD energy level  $\varepsilon_d$  localized approximately between chemical potentials of both leads (compare, for example, the curves calculated for  $\mu_L = 8$ ).

Fig. 13 presents the comparison of the  $d\langle j_L(t) \rangle/d\mu_L$  vs.  $\mu_L$  curves calculated for vanishing  $V_{RL}$  (left panels) and for  $V_{RL} = 10$  (right panels) for two different values of the amplitudes  $\Delta_L$  ( $\Delta_d = \Delta_L/2$ ,  $\Delta_R = 0$ ). At the vanishing value of  $V_{RL}$ , the shape of the curves is symmetrical in relation to the

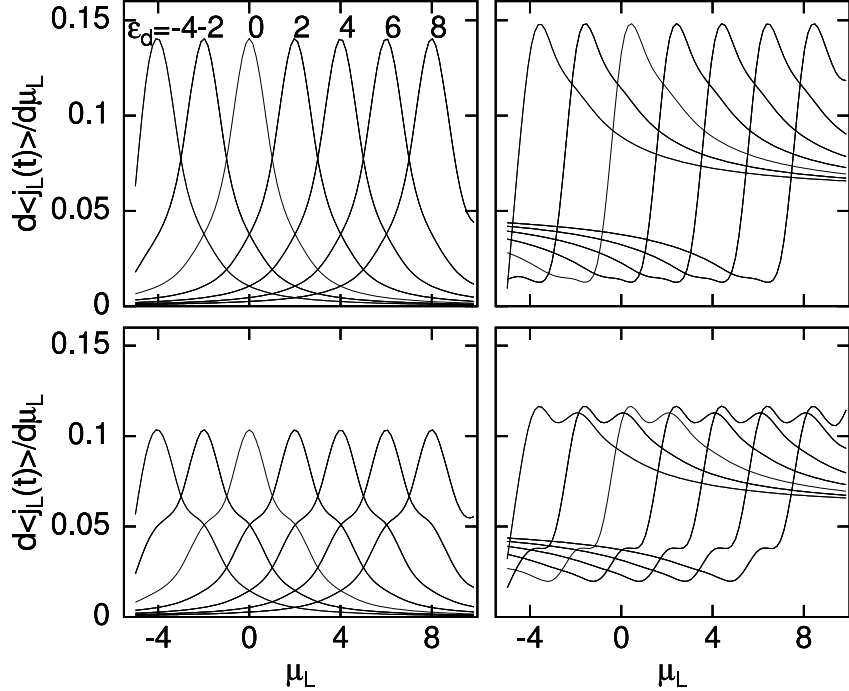


FIG. 13: The derivatives of the average current against  $\mu_L$  with respect to  $\mu_L$ ,  $d\langle j_L(t) \rangle / d\mu_L$ , for given values of  $\varepsilon_d$  (beginning from  $\varepsilon_d = -4$  up to  $\varepsilon_d = 8$ ). The left (right) panels correspond to  $V_{RL} = 0$  ( $V_{RL} = 10$ ) and upper (lower) panels correspond to  $\Delta_L = 2$  ( $\Delta_L = 4$ ). The other parameters as in Fig. 11. [9]

values  $\mu_L = \varepsilon_d$  although for greater  $\Delta_L$  some shoulders appear on both sides of the corresponding peaks in the distance  $\sim \Delta_L/2$  from the curve centers. For non-vanishing  $V_{RL}$ , the corresponding curves are approximately asymmetric and for large values of  $\mu_L$  they tend to constant, non-zero values corresponding to linear increasing of the current at large  $\mu_L$ . It is interesting that with the increasing amplitudes  $\Delta_L$  and  $\Delta_d$  very clear structures appear on both sides of the corresponding curves. Note, that all these curves can be obtained, for example, from the one calculated for  $\varepsilon_d = 0$  and moved along the  $\mu_L$ -axis by the corresponding value (equal to  $\varepsilon_d$ ).

Fig. 14 presents the average current  $\langle j_L(t) \rangle$  obtained for the case in which only the QD energy level  $\varepsilon_d$  oscillates with some frequency ( $\omega > \Gamma$ ) and for the small source-drain voltage  $\mu_L - \mu_R = 0.2$ . For vanishing  $V_{RL}$  (broken curves) we observe for small amplitude  $\Delta_d$  only a central resonant peak (Fig. 14a). With increasing  $\Delta_d$ , the subsequent peaks appear and the distance between them and the central peak is an integer multiple of the frequency  $\omega$  (side bands). The location of peaks is independent of the amplitude  $\Delta_d$  but their relative intensity values change and with increasing  $\Delta_d$  the height of the central peak is reduced. If we take the additional over-dot tunneling channel into consideration, especially for small  $\Delta_d$ , the asymmetric shape of the current curve is observed and this asymmetry increases with the increasing strength of the over-dot coupling between both leads. With the increasing amplitude  $\Delta_d$  this asymmetry is reduced largely due to the extra, photon-assisted tunneling peaks whose strength increases with the increasing  $\Delta_d$ .

As a last problem we consider the QD with the periodic rectangular-pulse external field applied to each QD-lead barrier. We assume that the influence of these fields on the system under consideration is equivalent to the following time-dependence of the matrix elements  $V_L$  and  $V_R$  corresponding to

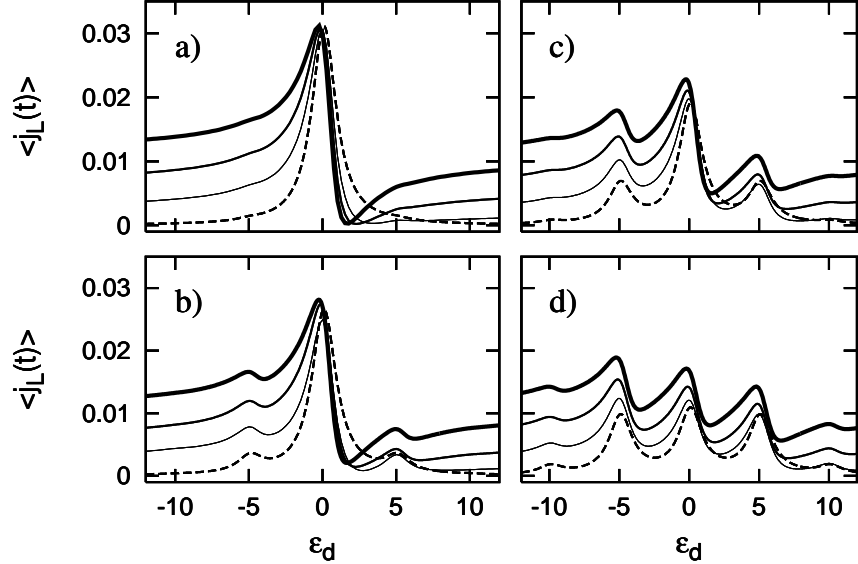


FIG. 14: The average current  $\langle j_L(t) \rangle$  against  $\varepsilon_d$  for the oscillating QD energy level at  $V_{RL} = 0, 4, 7, 10$  – broken, thin, thick and very thick curves, respectively. The panels a, b, c and d correspond to  $\Delta_d = 1, 3, 5$  and  $7$ , respectively.  $\omega = 5$ ,  $\Gamma = 1$ ,  $V = 4$ ,  $\mu_L = 0.2$ ,  $\Delta_L = \Delta_R = 0$ . [9]

the coupling of the QD with both leads:

$$\begin{aligned} V_L(t) &= 4, V_R = 0 \text{ for } 0 \leq t < T/2 \\ V_L(t) &= 0, V_R = 4 \text{ for } T/2 \leq t < T. \end{aligned}$$

The bridge tunneling channel is present all the time and the calculations were performed for  $V_{RL} = 4$  and  $V_{RL} = 10$ . In the upper part of Fig. 15 we show the time-dependence of  $V_L(t)$ . During the periodic coupling of the QD to the left or right lead the QD charge oscillates and the amplitude of these oscillations decreases with the increasing coupling  $V_{RL}$  between both leads. Note, that the greater  $V_{RL}$  enhances the equilibrium value of the QD charge at  $V_L = 0$  and  $V_R \neq 0$  (in the first half-period), but reduces it for  $V_L \neq 0$  and  $V_R = 0$  (i.e. in the second half-period). In two lower parts of Fig. 15 we show the current leaving the right and left leads for two values of the coupling  $V_{RL}$ . The effect of switching-on and -out of the QD-leads coupling on the currents is markedly visible. The time after which the currents achieve their steady values hardly depends on the coupling  $V_{RL}$ , although the width of the corresponding current peaks is smaller for lower values of  $V_{RL}$ .

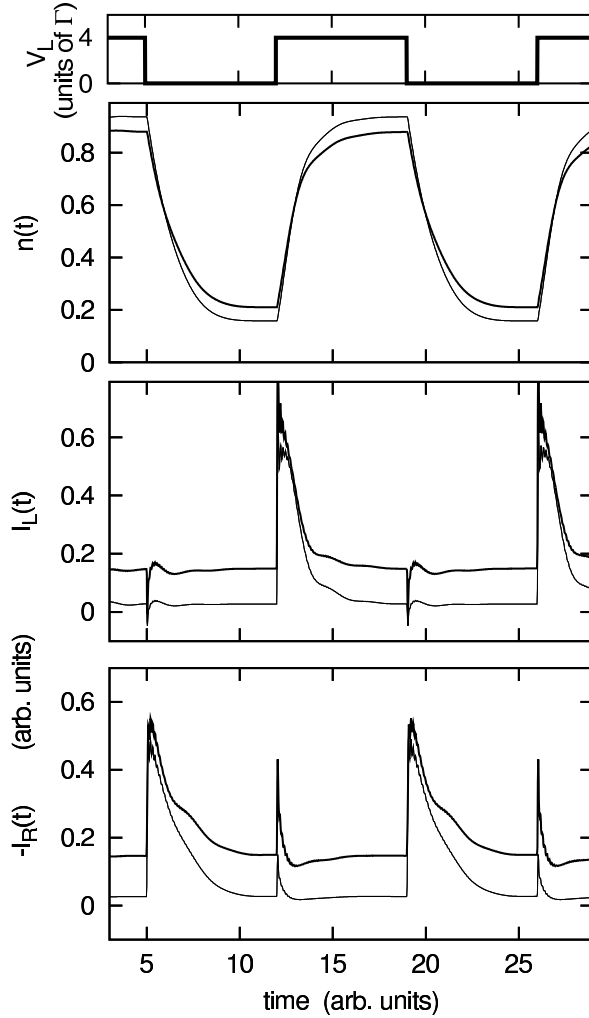


FIG. 15: The time-dependence of  $n(t)$ ,  $I_L(t)$  and  $I_R(t)$  for the case when the QD-lead barriers are changing in time as shown for  $V_L(t)$  in the upper panel ( $V_R(t)$  is out of phase with a phase difference of  $\pi$ ) for two values of the over-dot bridge tunneling channel strength corresponding to  $V_{RL} = 4$  (thin lines) and  $V_{RL} = 10$  (thick lines).  $\varepsilon_d = 1$ ,  $V = 4$ ,  $\mu_L = 4$ ,  $\mu_R = 0$ . [1]

#### IV. CONCLUDING REMARKS: IS ALL THIS RELATED TO QUANTUM INFORMATION PROCESSING?

The problems discussed here are of importance for small structures working at low temperatures. In such cases the presence of even single electron on the structure prevents other electrons to tunnel onto it. This is because small capacitance of these systems results in large charging energies which have been parametrised here by the Coulomb on dot repulsion.

As the ultimate goal of the miniaturisation is to build a quantum computer it maybe of interest to ask the question whether the systems considered will ever be used for this purpose. The answer is affirmative. It has been proposed to use charge [29] or spin [30] on a quantum dot to build a qubit – an elementary quantum unit of information. The subsequent work [31] has shown that the decoherence of a system consisting of two lateral quantum dots due to cotunneling does depend on the difference between chemical potentials of the two leads i.e. on the voltage. The future work will show whether the control of decoherence by the external bias will also be effective in more complex geometries.

**Acknowledgements:** This work has been partially supported by the grant no. PBZ-MIN-008/P03/2003 .

---

- [1] Kwapiński T, Taranko R., *Time-dependent transport through a quantum dot with the over-dot(bridge) additional tunneling channel* Physica **E 18** (2003) 402-411
- [2] Krawiec M, Wysokiński KI., *Nonequilibrium Kondo effect in asymmetrically coupled quantum dots* Phys. Rev. **B 66** 165408 (2002).
- [3] Kwapiński T, Taranko R, Taranko E., *Band structure effects in time-dependent electron transport through the quantum dot* Phys. Rev. **B 66** 035315 (2002).
- [4] Kwapiński T, Taranko R, Taranko E., *Time-dependent transport through a quantum dot: Mean-field, treatment of the Coulomb interaction* Acta Phys. Pol. **A 99** (2001) 293-305.
- [5] Krawiec M, Wysokiński KI., *Charge on the quantum dot in the presence of tunneling current* Solid State Commun **115** (2000) 141-144.
- [6] Krawiec M, Wysokiński KI., *Spectral functions of the quantum dot coupled to normal and/or superconducting leads* Acta Phys. Pol. **A 97** (2000) 197-200.
- [7] Krawiec M, Domański T, Wysokiński KI., *Do Van Hove singularities in leads influence tunneling current through quantum dot?* Acta Phys. Pol. **A 94** (1998) 411-414.
- [8] M. Krawiec, K. I. Wysokiński, *Electron transport through strongly interacting quantum dot coupled to normal metal and superconductor* Supercond. Sci. Technol. **17**, 103 (2004).
- [9] Taranko R., Kwapiński T., Taranko E., *Influence of microwave fields on the electron transport through a quantum dot in the presence of a direct tunneling between leads* arXiv:cond-mat/0304121 (2003) unpublished.
- [10] T. K. Ng and P. A. Lee, Phys. Rev. **61**, 1768 (1989); L. I. Glazman, and M. E. Raikh, Pis'ma Zh. Eksp. Teor. Fiz. **48**, 378 (1988) [Engl. transl. JETP] Lett. **47**, 452 (1988)]; S. Herschfield, J. H. Davies, and J. W. Wilkins, Phys. Rev. Lett. **67**, 3720 (1991).
- [11] Y. Meir N. S. Wingreen, and P. A. Lee, Phys. Rev. Lett. **70**, 2601 (1993); N. S. Wingreen, and Y. Meir, Phys. Rev. B **49**, 11040 (1994). Y. Meir N. S. Wingreen, P. A. Lee, Phys. Rev. Lett. **66**, 3048 (1991).
- [12] D. Goldhaber-Gordon, H. Shtrikman, D. Mahalu, D. Abusch-Magder, U. Meirav, M. A. Kastner, Nature **391**, 156 (1998).
- [13] S. M. Cronenwett, T. H. Oosterkamp, L. P. Kouwenhoven, Science **281**, 540 (1998).
- [14] J. Schmid, J. Weis, K. Eberl, K. von Klitzing, Physica **B256-258**, 182 (1998).
- [15] F. Simmel, R. H. Blick, J. P. Kotthaus, W. Wegscheider, M. Bichler, Phys. Rev. Lett. **83**, 804, (1999).
- [16] T. H. Oosterkamp, L.P. Kouwenhoven, A.E.A. Koden, N.C. van der Vaart, C.J.P.M. Harmans, Phys. Rev. Lett. **78**, 1536 (1997).
- [17] Qing-feng Sun, Tsung-han Lin, Phys. Rev. **B56** 3591 (1997).
- [18] Qing-feng Sun, Jian Wang, Tsung-han Lin, Phys. Rev. **B58**,13007 (1998).
- [19] C.A. Stafford, N.S. Wingreen, Phys. Rev. Lett. **76**, 1916 (1996).
- [20] Qing-feng Sun, Tsung-han Lin, J. Phys.: Condens. Matter **9**, 3043 (1997).
- [21] L.P. Kouwenhoven, A.T. Johnson, N.C. van der Vaart, A. van der Enden, C.J.P.M. Harmans, C.T. Foxon, Z. Phys. B, Condens. Matter **85**, 381 (1991).
- [22] H.-K. Zhao, J. Wang, Eur. Phys. J. **B9**, 513 (1999).
- [23] Y. Goldin, Y. Avishai, Phys. Rev. **B61**, 16750 (2000).
- [24] M. Tsukada, N. Shima, in: "Dynamical Processes and Ordering on Solid Surfaces", Eds. A. Yoshimori and M. Tsukada (Springer, Berlin 1995), p. 34; T.B. Grimley, V.C.J. Bhasu, K.L. Sebastian, Surf. Sci. **121**, 305 (1983).
- [25] J. Göres, D. Goldhaber-Gordon, S. Heemeyer, M.A. Kastner, H. Shtrikman, D. Mahalu, U. Meirav, Phys. Rev. **B62**, 2188 (2000).
- [26] M. Plihal, J.W. Gadzuk, Phys. Rev. **B63**, 085404 (2001).
- [27] V. Madhavan, W. Chen, T. Jamneala, M.F. Crommie, N.S. Wingreen, Science **280**,567 (1998).
- [28] O. Ujsaghy, J. Kroha, L. Szunyogh, A. Zawadowski, Phys. Rev. Lett. **85**, 2557 (2000).
- [29] J.A. Brum, P. Hawrylak, Superlattices and Microstructures, **22** 431 (1997).
- [30] D. Loss, D.P. Di Vincenzo, Phys. Rev. **A57** 120 (1998).
- [31] U. Hartmann, F.K. Wilhelm *Decoherence of charge states in double quantum dots due to cotunneling* arXiv:cond-mat/0208220.